Characterization of gallium oxide/glass thin films grown by RF magnetron sputtering

Soheil MOBTAKERİ [1] , *Ebru Şenadım TÜZEMEN* [2,3,*] , *Ali ÖZER* [4,5] , *Emre GÜR* [1]

[1]*Atatürk University, Department of Physics, 25250 Erzurum/TURKEY*

[2]*Sivas Cumhuriyet University, Nanophotonic Application and Research Center, 58140, Sivas/ TURKEY*

[3]*Sivas Cumhuriyet University, Department of Physics, 58140, Sivas/ TURKEY*

[4]*Sivas Cumhuriyet University, Department of Metallurgical and Materials Engineering, 58140, Sivas/ TURKEY*

[5]*Sivas Cumhuriyet University, Advanced Technology R&D Center, 58140, Sivas/TURKEY*

Abstract

In the present work, Gallium Oxide (Ga_2O_3) were deposited as thin films by radio frequency (RF) magnetron sputtering at 300 °C substrate temperature on glass substrate using Ga_2O_3 target with 99.99% purity. The crystalline structure, morphology, optical properties of the Gallium Oxide films were determined using X-ray diffraction (XRD), scanning electron microscopy (SEM) and UV–Visible Spectrometry, respectively. Experimental results show that annealing has an important role in the changes observed in the characterization of the Gallium Oxide thin films. All thin films produced were amorphous, except for the annealed P4-500. SEM pictures reveal the morphology of prepared Gallium Oxide thin films. The refractive index and real part of complex dielectric constant increased as the film deposition pressure increased.

1. Introduction

Gallium has many important compounds such as GaAs, GaN, InGaN. Since these compounds are semiconductor, they are used in many fields due to their electronic and optical properties. While GaAs are used in microwave circuits, ultraviolet applications, GaN and InGaN can be used in light emitting diodes. Another important compound of gallium is Gallium Oxide (Ga_2O_3). Gallium Oxide (Ga_2O_3) has five different crystal structures: α, β, γ, δ and ε. Stable obtainable phases are α and β phases. The β phase is the most chemically and thermally stable phase in all structures [1-3]. The β phase, which is a monoclinic structure [4], has attracted the attention of researchers due to its application areas arising due to its high features.

β -Ga_2O_3 shows an insulating property due to the wide band gap of 4.7-4.9 eV in atmospheric conditions, while it shows semiconductor properties over 500 °C (773 K) [5]. It can also be used to detect reducing gases at temperatures above 500 °C, and to detect oxygen gas at temperatures above 900 °C. It is used in UV

detectors because of its wide band gap range (4.7-4.9 eV), as it shows photoconductivity against deep UV [6-8]. Besides these; it has areas of use such as the original memory feature provided by the rotational magnetism of the transmitting electrons that function in the range of 4K to room temperature, as transmission conductive oxide in optoelectronic devices in coatings that do not reflect on GaAs [1, 2, 9].

The most commonly used methods are magnetron sputtering method [10, 11, 12], spray pyrolysis [5, 6, 13], sol-gel method [10], electron beam evaporation method [9,14,15] to produce Ga_2O_3 thin films. Especially in gas sensor applications, RF magnetron sputtering method is used. In this study, Gallium Oxide thin films were produced by RF magnetron sputtering method and structural and optical characterization was done.
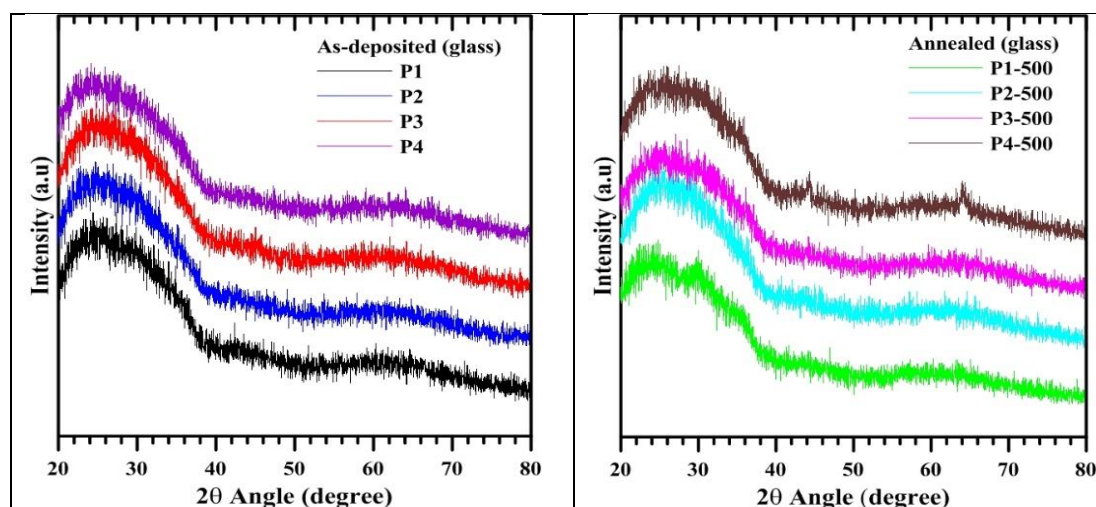
2. Experimental Details

2.1. Sample preparation

Ga_2O_3 thin films were deposited by RF magnetron sputtering on glass substrates using a Ga_2O_3 target (99.99% Pure, 2.00″ diameter × 0.125″ thick; Plasmaterials Inc.). The RF-sputtering parameters of Ga_2O_3 thin films were listed in Table 1. Glass substrates were firstly cleaned with acetone, isopropyl alcohol, and deionized water and then dried with air. Substrates were heated at 300 °C and distance between the target and substrate was adjusted to 7 cm. After placing each substrate in the chamber, the system was evacuated to a vacuum of the order of ~10^{-7} Torr using a turbo molecular pump. The Ga_2O_3 thin films produced were annealed at 500 °C. The magnetron sputtering of Ga_2O_3 thin films were deposited on glass substrates at the same condition but different deposition pressure and were labeled as P1 (7.50 mTorr), P2 (9.20 mTorr), P3 (10.40 mTorr), P4 (12.20 mTorr). The films Gallium Oxide annealed at 500 °C were named as P1-500 (7.50 mTorr), P2-500 (9.20 mTorr), P3-500 (10.40 mTorr), P4-500 (12.20 mTorr).

Table 1. The experimental deposition parameters of thin film coatings due to deposition pressure

	Growth Pressure (mTorr)	Ar (sccm)	Rotation (1 Rot)	Deposition Rate (Å/s)
P1	7.50	15	20 s	0.7-0.8
P2	9.20	45	20 s	0.8-0.9
P3	10.40	75	20 s	0.8
P4	12.20	105	20 s	0.8-0.9

2.2. Measurements

In this study, the direct influence of deposition pressure on the structural and optical properties of Gallium Oxide thin films are investigated. In order to investigate the crystalline properties, films were examined by X-ray diffraction (XRD) measurements. For XRD studies, a Rigaku Miniflex II Desktop X-ray Diffractometer system was used with Cu K$_\alpha$ radiation (λ= 1.54059 Å). Scanning electron microscopy (SEM) analysis was performed using TESCAN® MIRA3 XMU (Brno, Czechia) at an accelerating voltage of 10 kV. Optical characterization of the samples was carried out using a double-beam UV–Vis–NIR spectrophotometer (Cary 5000). Optical transmission spectra of the center point of samples were taken in the wavelength of 200–800 nm using solid sample holder accessory

3. Results and Discussion

3.1. X-ray diffraction (XRD)

The X-ray diffraction measurements of Ga_2O_3 thin films produced on glass substrates were measured with Rigaku Miniflex II Desktop X-ray Diffractometer system. The X-ray diffraction of the films produced at different growth pressures are shown in Fig. 1. Diffraction patterns were obtained in the range of $2\theta = 20\text{-}80°$.

Figure 1. XRD spectra for as-deposited and annealed Ga_2O_3 films deposited different deposition pressure

In Fig. 1, there is no signature peak observed at as-deposited thin films. The hump structure of amorphous silicate glass was observable without any peaks. Besides, there were no significant peaks of sputtered and grown materials. This indicates that the Ga_2O_3 films grown at a substrate temperature of 300 °C were amorphous. After annealing at 500 °C, while P1-500, P2-500, P3-500 are amorphous, the diffraction peaks are seen in P4-500. Annealing can reduce film internal stress, which can improve film crystallinity. Crystallinity of sample P4-500 annealed at 500 °C is better among films illustrated in Fig. 1.

The peaks observed at diffraction angles of 44.2 and 64.2°. The peaks observed at diffraction angles of 2θ =44.2° and 2θ= 64.2° correspond to the $\beta(-211)$ and $\beta((402))$ [JCPDS-11-0370] planes of Ga_2O_3, respectively.

3.2. Scanning electron microscopy (SEM)

As illustrated in Fig. 2, the increased pressure from P1 to P4 both for as-deposited and annealed conditions, the nuclei of Ga_2O_3 coated on glass substrates is observable.
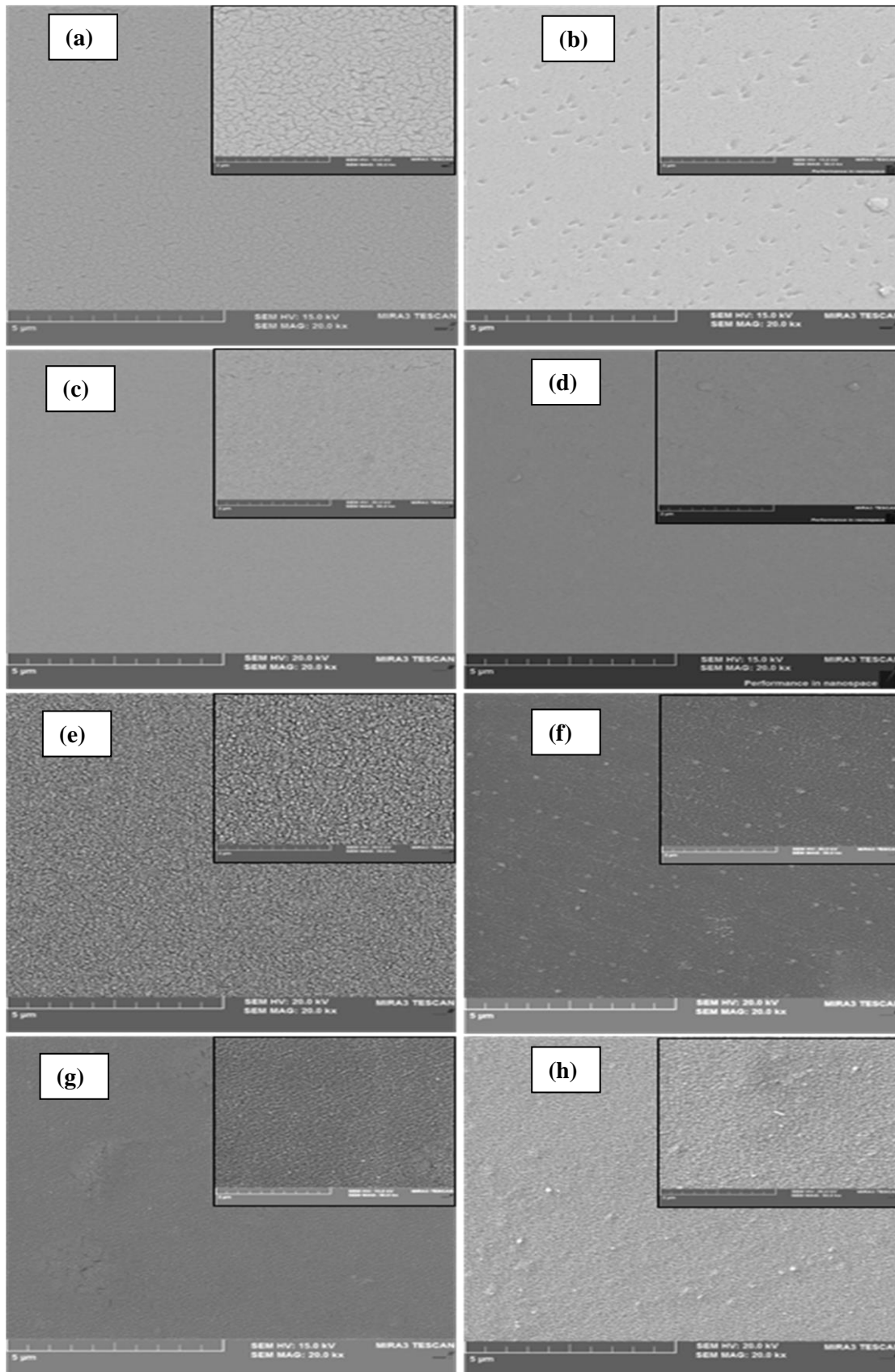
Figure 2. SEM patterns of Ga_2O_3 thin films as-deposited and annealed for 1 h at 500 °C by RF magnetron sputtering at various sputtering pressures on glass substrate a) as-deposited P1, b) annealed P1, c) as-deposited P2, d) annealed P2, e) as-deposited P3, f) annealed P3, g) as-deposited P4, h) annealed P4.

The growth and nucleation of seeds were developed up to about 100 and 125 nm for P3 and P4, respectively. The first row of Fig. 2(a) shows the deposited layer of Ga_2O_3 on glass under the lowest pressure that produced a porous layer of unannealed condition without any nucleation. The nucleation and growth of Ga_2O_3 by annealing Fig. 2(b), the pores get together to leave a bigger porous structure of about 100-150 nm due to the coarsening phenomenon while the grains get bigger as well while the pores behave as triangle-like pores among the growth grains. P2 (Fig. 2(c-d)) shows the best developed and well-distributed structure of similar grains both for as-deposited and annealed conditions. P3 in as-deposited condition (Fig. 2(e)), the well distributed grains are observable. After annealing (Fig. 2(f)), the grains were agglomerated in certain regions along the perpendicular direction which is the coating direction from upper left to lower right direction seen as droplets. Increasing pressure deteriorates the coating and coarsening of grains was random in some regions, the grain agglomerate size increased up to 140-160 nm, so that the properties may be destroyed by increased roughness which can refract the light. P4 with the highest pressured coating, in as-deposited condition

(Fig. 2(g)), some regions are seen as non-interacted layers of Ga_2O_3. This is seen as humped and cracked regions of coating, after annealing (Fig. 2(h)), the grains were coarsened up to 160-220 nm and some cracked regions are evident which may end up with agglomeration and humps. As a result, we can say that the highest pressure has the highest energy for adhesion to the surface.

3.3. Optical properties

The transmittance (T%) of the films obtained at different deposition pressures were measured at room temperature with Cary 5000 UV-VIS-NIR spectrophotometer with wavelength in the range of 175–3300 nm. In order to ensure that are independent of the underfloor absorption of the optical transmittance values of the films during these measurements, the ground correction was made firstly measuring the glass-to-glass transmittance. The graph of wavelength against transmittance of Ga_2O_3 thin films obtained at different deposition pressures is given in Fig. 3.
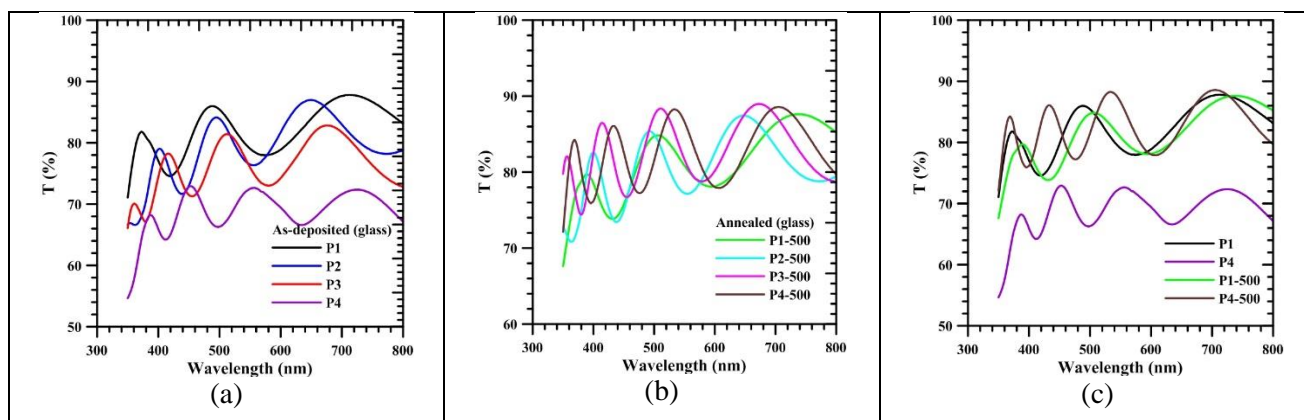
Figure 3. Transmittance spectra for a) as-deposited Ga_2O_3 films deposited different deposition pressure, b) annealing Ga_2O_3 films deposited different deposition pressure, c) as-deposited and annealing P1 and P4 Ga_2O_3 films

Fig. 3(a) shows that when pressure increases from 7.50 mTorr to 12.20 mTorr, transmittance decreases. In this case, it is possible to say that the amount of Ga increases as the pressure increases. When Ga_2O_3 films were annealed at 500 °C, it was observed that the transmittance increased in four samples. Specifically, the P4 sample with 12.20 mTorr showed an extremely significant increase after annealing. In other words, while it had 72% transmittance before annealing, it increased to about 88% after annealing (Fig. 3(c)).

Using the transmittance graphs in Fig. 3, the thicknesses of the Ga_2O_3 films were calculated.

Interference fringes of transmittance were used to find of thickness. Using the wavelengths and refractive index values between two adjacent maxima or minima, thickness values are calculated with the help of the following equation.

$$d = \left\{ 2 \left[\frac{n(\lambda_1)}{\lambda_1} - \frac{n(\lambda_2)}{\lambda_2} \right] \right\}^{-1} \tag{1}$$

In this study, the refractive index was taken as n = 1.91 [16]

The thicknesses calculated from the transmittance curves can be seen in Table 2. Both before and after annealing, it was observed that the thicknesses

increased as the pressure increased. We can think that it is the result of the increase of Ga amount which in turn may increase the O amount to produce stable Ga_2O_3 as indicated in XRD results as pressure increases.

Table 2. Thickness for as-deposited and annealing Ga_2O_3 films deposited different deposition pressure

Thickness (nm)	P1	P2	P3	P4
As-deposited	408.5	548.7	579.67	608.9
Annealing	408.5	548.7	553.8	577.3

Absorption coefficients values of Ga_2O_3 thin films grown at different pressures were calculated using the following equation [17].

$$\alpha = \frac{1}{d}Ln(1/T) \tag{2}$$

Here T shows the value of the light passing (transmission) and d shows the thickness of the film. According to Tauc et al. [18], it is possible to separate different regions in the absorption edge spectrum. An exponential part called Urbach's tail near the edge of the optical band appears in poor crystalline, the disordered and amorphous materials, low-crystalline.

Such materials have localized states that lie in the band gap. In the exponent edge where the absorption coefficient lies in the absorption region of $1<\alpha<10^4 cm^{-1}$, the absorption coefficient is governed by the relation [19],

$$\alpha = AE_0^{3/2}\exp\left(\frac{h\nu}{E_0}\right) \; for \; h\nu < E_g \tag{3}$$

Where E_0 is an empirical parameter describing the width of the localized states in the band gap due to above mention effects. As in a material increases disordered, we can say that its Urbach energy will increase. The value of Urbach tail energy (E_0) is calculated from the slope of this the linear plot. Urbach Energy values were found by using Fig. 4. These values are shown in Table 3. As can be seen from the calculated Urbach energies, Urbach energies of thin films depend on the effect of annealing decreases. Because of the thin film annealing particle size increases and their disordere decreases. Therefore, the value of Urbach energies has decreased. We can say that there is an improvement in the quality of the Ga_2O_3 films by annealing. This is particularly evident in P4 and P4-500 films.
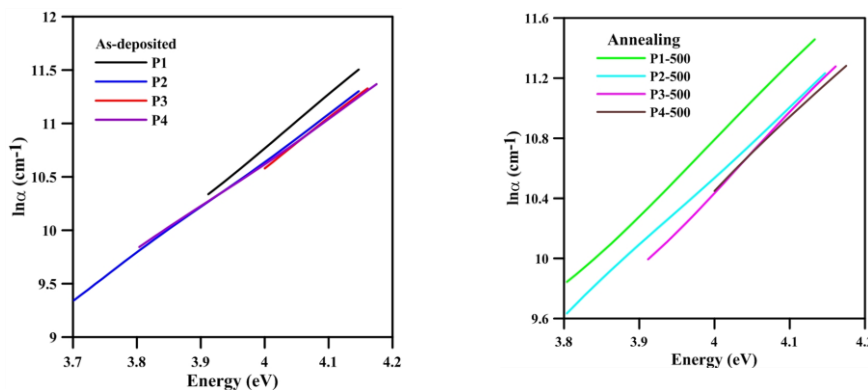
Figure 4. Photon energy-dependent variation of $\ln\alpha$ in Ga_2O_3 thin films produced at different pressures.

Table 3. Urbach tail energy (band tail energy) E_0 parameter for as-deposited and annealing Ga_2O_3 films deposited different deposition pressure

Urbach tail E_0 parameter (meV)	P1	P2	P3	P4
As-deposited	544.3	647.1	581.5	704.0
Annealing	541.9	584.5	500.8	477.5

In this study, the refractive index was determined using the Swanepoel method [20, 21]. In order to use this method, interference effects in the transmittance curve are used. Using the transmittance curve, the top and bottom envelopes were drawn. The refractive indices of the films were found from the formula below.

$$n = [N + (N^2 - n_s^2)^{1/2}]^{1/2} \tag{4}$$

$$N = \frac{(n_s^2+1)}{2} + 2n_s\frac{(T_{max}-T_{min})}{T_{max}T_{min}} \tag{5}$$

The representation of the envelope for the simulated P2-500 transmittance curve, passing through the maximum of the spectrum (T_{max}) and the minimum of the spectrum (T_{min}), is shown in Fig. 5(a).
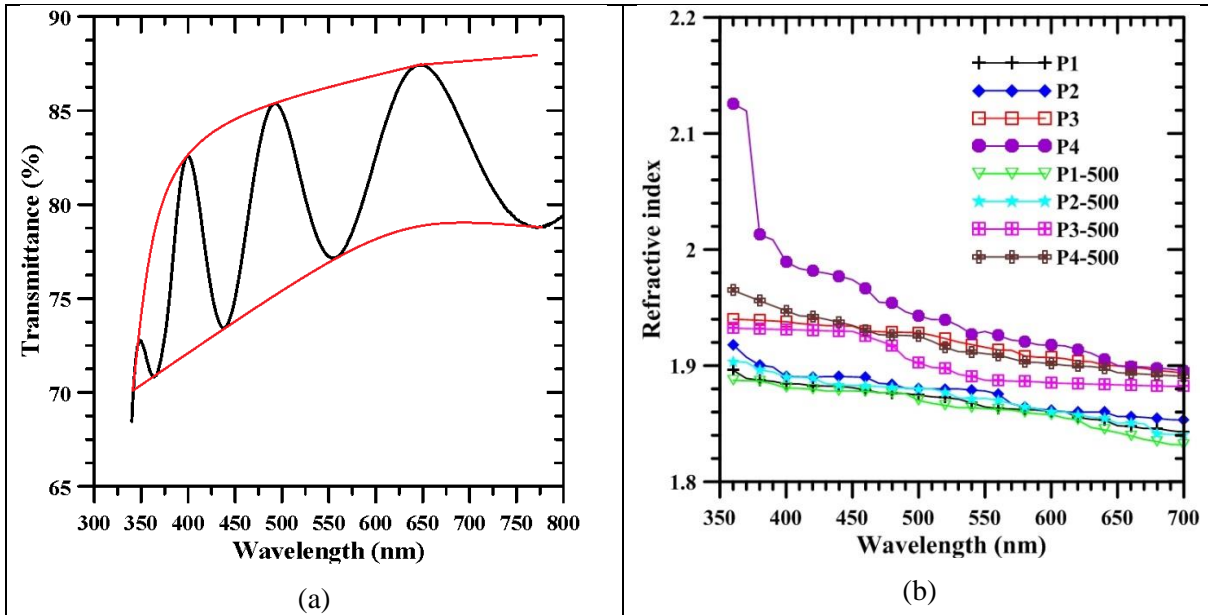
Figure 5. a) Swanepoel method for P2-500 film and b) At various sputtering pressures refractive index vs. wavelength plots for as-deposited and annealed films

For all non-annealed and annealed Ga₂O₃ films, the procedure performed in Fig. 5(a) was performed and refractive indices were found using the equations nearby. As seen in Fig. 5(b), the refractive index values of Ga₂O₃ films were determined to decrease with decreasing pressure in the visible region. The decrease in refractive index with decreasing pressure is thought to be caused by the decrease in the packing density.

The basic excitation spectrum of the films can be defined by expressing the frequency dependence of the complex dielectric constant. The real and imaginary part of the dielectric constant depends on n and k values. The real and imaginary part of the dielectric constant is determined by the following equations [22,23]:
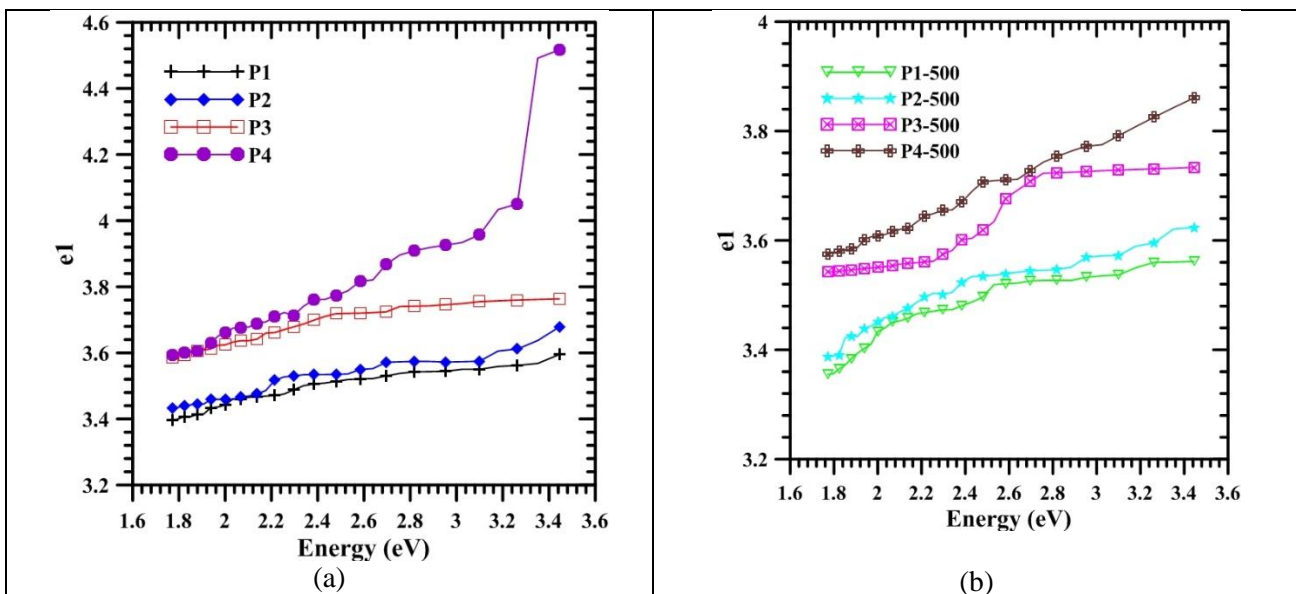
$$\varepsilon_1 = n^2 - k^2 \tag{6}$$

$$\varepsilon_2 = 2nk \tag{7}$$

Here ε_1 denotes the real part, ε_2 denotes the imaginary part. The extinction coefficient (k), depending on absorption coefficient (α)

$$k = \frac{\alpha \lambda}{4\pi} \tag{8}$$

determined by its relation.

Figure 6. At various sputtering pressures the real part of the dielectric constant vs. energy plots for a) as-deposited and b) annealed films

Fig. 6 shows the change of real dielectric constants of Ga_2O_3 thin films produced on glass at different sputtering pressures. The real dielectric constants of the as-deposited and annealed thin films increase as the pressure increases. These results are compatible with the literature [24].

4. Conclusions

Ga_2O_3 thin films were obtained at different deposition pressures by RF magnetron sputtering method on glass substrate. The films deposited were annealed at 500°C in the air. The effects of structural and optical properties of these films on pressure were examined. Crystallinity of sample P4-500 annealed at 500 °C is better among films. When Ga_2O_3 films were annealed at 500°C, it was observed that the transmittance increased in all samples and thicknesses increased as the pressure increased. The refractive index values of Ga_2O_3 films were determined to decrease with decreasing pressure in the visible region. The real dielectric constants of the as-deposited and annealed thin films increase as the pressure increases. In this study, the surface structures of all samples were investigated by scanning electron microscopy. Differences in particle structure were observed with increasing pressure.

Acknowledgement

Conflicts of interest

The authors state that did not have conflict of interests.

References

[1] Litimein F., Rached D., Khenata R., Baltache H., FPLAPW study of the structural, electronic and optical properties of Ga_2O_3: Monoclinic and hexagonal phases, *Journals of Alloys and Compounds*, 488 (2009) 148-156.

[2] Machon D., McMillan P. F., Xu B., Dong J., High pressure study of the β-to-α transition in Ga_2O_3, *Physical Review B*, 73 (2006) 094125.

[3] Zinkevich M., Aldinger F., Thermodynamic Assessment of the Gallium-Oxygen System, *Journal of the American Ceramic Society*, 87 (2004) 683-691.

[4] Geller S., Crystal structure of β-Ga_2O_3, *The Journal of Chemical Physics*, 33 (1960) 676-684.

[5] Ortiz A., Alonso J. C., Andrade E., Urbiola C., Structural and Optical Characteristics of Gallium Oxide Thin Films Deposited by Ultrasonic Spray Pyrolysis, *Journal of The Electrochemical Society*, 148 (2001) F26-F29.

[6] Ji Z., Du J., Fan J., Wang W., Gallium oxide films for filter and solar-blind UV detector, *Optical Materials*, 28 (2006) 415-417.

[7] Kokubun Y., Miura K., Endo F., Nakagomi S., Sol-gel prepared β-Ga_2O_3 thin films for ultraviolet photodetectors, *Applied Physics Letters*, 90, (2009) 031912: 1-031912:3.

[8] Oshima T., Okuno T., Arai N., Suzuki N., Hino H., Fujita S., Flame Detection by a β-Ga_2O_3-Based Sensor, *Japanese Journal of Applied Physics*, 48 (2009) 011605: 1-011605:7.

[9] Al-Kuhaili M. F., Durani S. M. A., Khawaja E. E., Optical properties of gallium oxide films deposited by electron-beam evaporation, *Applied Physics Letters*, 83 (2003) 4533-4535.

[10] Miyata T., Nakatani T., Minami T., Manganese-activated gallium oxide electroluminescent phosphor thin films prepared using various deposition methods, *Thin Solid Films*, 373 (2000) 145-149.

[11] Fleischer M., Meixner H., Characterization and crystallite growth of semiconducting high-temperature stable Ga_2O_3 thin films, *Journal of Materials Science Letters*, 11 (1992) 1728-1731.

[12] Marie P., Portier X., Cardin J., Growth and characterization of gallium oxide thin films by radiofrequency magnetron sputtering, *Physica Status Solidi (a)*, 205 (2008) 1943-1946.

[13] Hao J., Lou Z., Renaud I., Cocivera M., Electroluminescence of europium doped gallium oxide thin films, *Thin Solid Films*, 467 (2004) 182-185.

[14] Oldham N. C., Hill C. J., Garland C. M., McGill T. C., Deposition of Ga_2O_3-x ultrathin films on GaAs by e-beam evaporation, *Journal of Vacuum Science and Technology A: Vacuum, Surfaces, and Films*, 20 (2002) 809-813.

[15] Passlack M., Hunt N. E. J., Schubert E. F., Zydzik G. J., Hong M., Mannaerts J. P., Opila R. L., Fischer R. J., Dielectric properties of electron-beam deposited Ga_2O_3 films, *Applied Physics Letters*, 64 (1994) 2715-2717.

[16] Li X., Lu H. L., Ma H. P., Yang J. G., Chen J. X., Huang W., Guo Q., Feng J. J., Zhang D. W., Chemical, optical, and electrical characterization of Ga_2O_3 thin films grown by plasma-enhanced atomic layer deposition, *Current Applied Physics*, 19 (2019) 72-81.

[17] Qiang S., Qingru W., Dong Z., Qinglin W., Shuhong L., Wenjun W., Quli F., Junying Z., Structural, optical and photoluminescence properties of Ga_2O_3 thin films deposited by vacuum thermal evaporation, *Journal of Luminescence*, 206 (2019) 53-58.

[18] Tauc J., Grigorovici R., Vancu Y., Optical Properties and Electronic Structure of Amorphous Germanium, *Phys. Status Solidi*, 15 (1966) 627-637.

[19] Pankove J. I., Absorption Edge of Impure Gallium Arsenide, *Phys. Rev.*, 140 (1965) A2059-A2065.

[20] Soliman L. I., Ibrahim A. M., Determination of optical constants of thermally evaporated CdS_xSe_{1-x} thin films using only transmission spectra, *Fizika A*, 6 (1997) 181-188.

[21] Won D. J., Wang C. H., Jang H. K., Choi D. J., Effects of the thermally induced anatase-to-rutile phase transition in MOCVD-grown TiO_2 films on structural and optical properties, *Appl. Phys. A*, 73 (2001) 595-600.

[22] Senadım E., Eker S., Kavak H., Esen R., Optical and structural parameters of the ZnO thin film grown by pulsed filtered cathodic vacuum arc deposition, *Solid State Communications*, 139 (2006) 479-484.

[23] Senadım Tuzemen E., Eker S., Kavak H., Esen R., Dependence of film thickness on the structural and optical properties of ZnO thin films, *Applied Surface Science*, 255 (2009) 6195-6200.

[24] Higashiwaki M., Fujita S., Gallium Oxide: Materials Properties, Crystal Growth, and Devices, 2020 Edition (Springer Series in Materials Science) 1st ed. Print ISBN: 978-3-030-37152-4 Electronic ISBN: 978-3-030-37153-1